Mobilizing sorghum genetic diversity: Biochemical and histological-assisted design of a stem ideotype for biomethane production

Hélène Laurence Thomas, David Pot, Sylvie Jaffuel, Jean-luc Verdeil, Christelle Baptiste, Laurent Bonnal, Gilles Trouche, Denis Bastianelli, Eric Latrille, Angélique Berger, et al.

Received: 23 March 2021 | Revised: 9 July 2021 | Accepted: 18 July 2021

DOI: 10.1111/gcbb.12886

GCB-BIOENERGY BIOPRODUCTS FOR A SUSTAINABLE BIOECONOMY Open Access

WILEY

ORIGINAL RESEARCH

Mobilizing sorghum genetic diversity: Biochemical and histological-assisted design of a stem ideotype for biomethane production

Hélène Laurence Thomas[1] | **David Pot**[2,3] | **Sylvie Jaffuel**[2,3] | **Jean-Luc Verdeil**[2,3] | **Christelle Baptiste**[2,3] | **Laurent Bonnal**[4,5] | **Gilles Trouche**[2,3] | **Denis Bastianelli**[4,5] | **Eric Latrille**[1] | **Angélique Berger**[2,3] | **Caroline Calatayud**[2,3] | **Céline Chauvergne**[1] | **Virginie Rossard**[1] | **Patrice Jeanson**[6] | **Joël Alcouffe**[7] | **Hélène Carrère**[1]

[1]INRAE, Univ Montpellier, Narbonne, France

[2]CIRAD, UMR AGAP Institut, Montpellier, France

[3]UMR AGAP Institut, Univ Montpellier, CIRAD, INRAE, Institut Agro, Montpellier, France

[4]CIRAD, UMR SELMET, Montpellier, France

[5]SELMET, Univ Montpellier, CIRAD, INRAE, Institut Agro, Montpellier, France

[6]EUROSORHO, Mondonville, France

[7]RAGT2N, Rivières, France

Correspondence
David Pot, CIRAD, UMR AGAP, TA A-108 / 03, Avenue Agropolis, F-34398 Montpellier Cedex 5, France.
Email: david.pot@cirad.fr

Funding information
Agence Nationale de la Recherche, Grant/Award Number: ANR-11-BTBR-0006-BFF

Abstract

Sorghum currently contributes to the species portfolio that is supporting bioenergy production including anaerobic digestion. Although agro-morphological ideotypes maximizing biogas production have been recently proposed, there is a crucial need to refine our understanding of the impacts of the stem composition and structure on this processing trait in order to ensure genetic gains in the mid to long terms. This study aims to assess the potential of *Sorghum bicolor ssp bicolor* stem genetic diversity to maximize genetic gains for biogas production and define a biogas stem ideotype. In this context, a panel of 57 genotypes, encompassing most of the stem composition variability available in cultivated sorghum, was characterized over five sites. Simultaneous histological and biochemical characterizations were performed. A high broad sense heritability associated with a moderate genetic variability was detected for stem biogas potential ensuring significant genetic gains in the future. In addition, the development of a stem histological phenotyping pipeline made it possible to describe the genetic diversity available for the internode anatomy and the repartition of key cell wall components. Consistently with previous studies, moderate to high heritability was observed for stem biochemical components. Genetic correlation, hierarchical clustering, and multiple stepwise regression analyses identified soluble sugar content as the first main driver of biogas potential genetic variability. Nevertheless, breeding programs should anticipate that biogas yield improvement will also rely on the monitoring of the cell wall components and their distribution in the stem jointly with the soluble sugar content. According to the assets of sorghum in terms of adaptation to environmental

David Pot and Hélène Carrere should be considered joint senior authors.

stresses and the present results regarding the identification of stem ideotypes suitable for different value chains, this species will surely play a key role to optimize the economic and environmental sustainability of the agrosystems that are currently facing the effects of climate change.

KEYWORDS

anaerobic digestion, animal feed, combustion, genetic diversity, heritability, ideotype, internode anatomy, sorghum, stem composition

1 | INTRODUCTION

The relevance of sorghum as a feedstock to support bioenergy production has been underlined at the economic and environmental levels in the United States (Cai et al., 2013; Fertitta-Roberts et al., 2017; Fulton-Smith and Cotrufo, 2019; Gautam et al., 2020; Moore et al., 2021; Oikawa et al., 2015), China (Liu et al., 2015), Latin America (Almeida et al., 2019; Rezende & Richardson, 2017), Africa (Vries et al., 2012), and Europe (Jankowski et al., 2020; Shu et al., 2020; Szambelan et al., 2018; Vlachos et al., 2015). Jointly with its use in starch and soluble sugar-based first-generation ethanol production (Szambelan et al., 2018), sorghum vegetative parts or even whole plants can also be used in second-generation ligno-cellulosic-based ethanol (Almeida et al., 2019; Mitchell et al., 2016; Rooney et al., 2007) or anaerobic digestion (Barbanti et al., 2014; Pasteris et al., 2021; Shoemaker & Bransby, 2010; Thomas et al., 2017), taking advantage of their structural carbohydrates reservoir. In addition to these biochemical processes, the thermochemical routes (including combustion) also constitute possible strategies to ensure energy autonomy at various geographical scales.

Sorghum success is mainly due to its high level of drought tolerance (Zegada-Lizarazu et al., 2015), its high nutrients use efficiency (Hao et al., 2014), and its adaptation to a large array of environmental conditions, cropping systems (sorghum can be cultivated as a main or second crop as exemplified for methane production by Garuti et al., (2020)) and uses. Sorghum genotypes with high biomass potentials and suitable to support the development of biomass value chains in temperate (Amaducci et al., 2016) and semi-arid environments (Oikawa et al., 2015) have already been identified. Sorghum also presents a large phenotypic diversity regarding biomass composition (Brenton et al., 2016; Niu et al., 2020; Trouche et al., 2014) that constitutes a vector of adaptation to diverse biomass value chains.

Among the different energy production processes, the development of anaerobic digestion is expected to contribute significantly to energy autonomy at local level (Bourdin & Nadou, 2020) and to greenhouse gas emissions reduction (Brémond et al., 2020). Maximization of methane production yield through the development of sorghum varieties targeting specifically this value chain is possible. It has been shown that sorghum genotypes harbor different abilities to produce methane (Mahmood & Honermeier, 2012; Mahmood et al., 2013; Pasteris et al., 2021; Thomas et al., 2017; Windpassinger et al., 2015). In this context, optimization of breeding efforts requires a better definition of the sorghum biomethane ideotype to target. Previous works highlighted that the main driver of energy yield per hectare (either methane, ethanol, or calorific energy) corresponds to the dry matter yield per hectare (Carvalho & Rooney, 2017; Garuti et al., 2020), although an alternative biogas ideotype characterized by high contributions of panicles to total dry matter and accepting a lower dry biomass potential was also proposed (Windpassinger et al., 2015). Nevertheless, as breeding is an anticipation exercise, there is a pressing need to identify which traits will be able to maximize energy production within these agro-morphological ideotypes.

It has already been shown that the primary components of non-structural carbohydrates in sorghum are sucrose, fructose, glucose, and starch and that significant genetic variations are available for these traits as well as for the cell wall-related ones (Saballos, 2008). In addition, it is well known that the biochemical composition of the cell wall impacts methane yield (Monlau et al., 2012) through its effects on the hydrolysis potential of the lignocellulosic biomass. Nevertheless, up to now, studies dealing with sorghum biomethane production mainly analyzed the impacts of whole aboveground biomass yield, organ proportions (Windpassinger et al., 2015), and whole plant biomass quality on methane yield (Pasteris et al., 2021) whereas they did not directly address the contributions of the stem biochemical and histological properties to the methane yield. As these two types of traits can have complementary impacts on the degradability of the biomass, there is an obvious interest to clarify their specific effects on methane production potential and determine, if these effects are significant, a stem sorghum ideotype to maximize methane production potential.

Models at the intraspecific level were developed to predict the yield of different bioconversion processes

involving enzymatic hydrolysis. Vandenbrink et al., (2010) used a panel of 381 field-grown sorghum varieties to study whole plant enzymatic hydrolysis yield and El Hage et al., (2018) used 11 maize inbred lines to study cell wall digestibility variability. This last study incorporated the use of internode histological traits to improve the description of the stem biomass properties. Moreover, this study highlighted that stem is the most important contributor to the whole aboveground maize biomass. The same holds true in the case of high-yielding biomass sorghum hybrids for which a panicle/stem ratio of 1:10 and a leaf/stem ratio of 1:4.5 were observed (Windpassinger et al., 2015). In addition, analyzing tissue-specific hydrolysis yield in sorghum, Vandenbrink et al., (2013) underlined the highest performances of stems in relation to the leaves and suggested that the development of biomass varieties should prioritize the maximization of stem biomass yield. To the best of our knowledge, no study aimed to precisely define a sorghum stem biochemical and histological ideotype that would maximize biomethane yield in order to support breeding efforts.

The first aim of this study was to determine if the stem methane potential can be optimized by taking advantage of the genetic variability available for this trait. The second aim was to explore the genetic correlations of biochemical and histological stem properties with stem biomethane potential in order to define a stem ideotype specifically targeting this processing trait. Third, the relationships between biomethane potential, in vitro dry matter digestibility, and higher heating value (a proxy for combustion) and their specific determinants were analyzed to define whether different ideotypes should be developed for these targets.

2 | MATERIALS AND METHODS

2.1 | Plant material and experimental designs

A total of 57 genotypes were included in this study (Table S1). This panel (Panel57) encompasses 33 landraces that cover the five main sorghum races and include three converted landraces from the US Sorghum Association Panel (Casa et al., 2008). Breeding materials were also considered encompassing 20 genotypes originating from US Universities, EUROSORGHO, RAGT2N, and CIRAD breeding programs. These 20 genotypes include 15 parental lines and 5 experimental hybrids. In addition, four commercial hybrids were considered. This panel covers the six genetic clusters that have been identified by Bouchet et al (2012) who analyzed a core collection encompassing sorghum worldwide diversity. The accessions were also selected to maximize their genetic variability at the stem biochemical level according to the study of Trouche et al., (2014). In addition, the panel was enriched in breeding and commercial material corresponding to the double purpose and industrial ideotype targets.

These genotypes were grown in five experimental trials located in three sites of the Occitanie region (France) between 2012 and 2014. The three sites correspond to Montpellier (MPL, France, 43°39′02″N 3°52′35″E, highly calcareous clay-loam soil), Mondonville (MDN, France, 43°40′41″ N 1°17′12″ E, calcareous clay-loam), and Rivières (RIV, France, 43°55′16″N 1°59′34.87″ E, calcareous clay-loam). The patterns of water inputs and temperature evolution for the five experiments are provided in Figure S1. The number of genotypes evaluated in each trial varied between 23 and 30 (Table S1). In order to limit competition between genotypes, they were established in the field according to their expected biomass production. Only one plot per genotype (an individual plot corresponding to 2–4 rows of 4–5 meters (depending on the considered trial) spaced at 0.6 m, with 18 seeds per linear meter) per experimental trial was produced and analyzed. For all the trials, the plants were harvested at the silage stage (dough grain). For all the genotypes, shoots originating from six healthy plants were harvested. The stems were separated from the leaves, tillers and panicles and crushed using a garden shredder VIKING GE335. The fresh ground material obtained was then dried at 60°C for 72 h. After drying, samples were grinded with a cutting mill (SM100, Retsch) with a 1-mm sieve to provide samples for biochemical characterization. At the same developmental stage, on the three trials established in Montpellier, four (MPL2014) to six (MPL2012, MPL2013) healthy additional plants were harvested for histological analyses. In MPL2012, the second internodes below the flag leaf were harvested whereas in MPL2013 and MPL2014, the fourth internodes below the flag leaf were harvested (Table S2). The stem and internode samples were then characterized at the histological, biochemical, and processing levels. A description of the traits is provided in Table S3.

2.2 | Determination of histological traits at the internode level

As described in Perrier et al., (2017), sorghum internodes were transversely cut with a thickness of 90 μm, then stained with FASGA. This staining method allows to highlight internode regions with high lignin content (cell walls stained in red) and with high holocellulose content (cell walls stained in blue) (Tolivia & Tolivia, 1987). Based on this coloration, the area of the outer zone Z1 in % of the internode section area (percZ1), the percentage

of sclerenchyma tissue in the outer zone Z1 in % of Z1 area (percSclZ1), the percentage of blue tissue in the inner region (Z2) of the internode in % of Z2 area (percBluZ2), the number of vascular bundle (VB) in the inner region Z2 (nbVBZ2), and the density in vascular bundles (densVBZ2) in the same region were recorded.

2.3 | Biochemical composition of the stem

Biochemical compositions of stem samples were estimated by NIRS (near-infrared spectroscopy) using a NIR system 6500 spectrometer (FOSS NirSystem). The calibrations available are based on whole aboveground biomass and stem samples (previously prepared as indicated in 2.1) that were analyzed using reference methods. Accuracies of prediction models including their R^2, SEC (Standard Error of Calibration), and SECV (Standard Error of Cross-Validation) are provided in Table S3. Total mineral content (MM, mineral matter or ash) was determined by igniting at 550°C. Crude protein (CP) content was estimated from the total nitrogen content (N) measured by Kjeldahl method, with the relationship CP = N* 6.25. Crude fiber content (CF) was derived according to the Weende method AAFCO 004.00. Soluble sugar fraction (SS) of the dry matter was estimated using the Luff Schoorl method. Fiber composition was assessed according to the sequential method of Van Soest et al., (1991) which measures neutral detergent fiber (NDF, AAFCO 009.07), acid detergent fiber (ADF, AAFCO 008.02), and acid detergent lignin (ADL) contents. Based on these results, hemicellulose (HEMI = NDF-ADF) and cellulose (CEL = ADF-ADL) contents were calculated. In addition, fiber fractions were also expressed as proportions of NDF, in order to characterize the quality of the fiber per se independently of the soluble carbohydrate and NDF that largely impact their absolute values. These additional variables were calculated as follows: for cellulose: CVS_in_NDF = CEL/NDF*100, for hemicellulose: HEMI_in_NDF = HEMI/NDF*100, and for lignin: ADL_in_NDF = ADL/NDF*100.

2.4 | Characterization of processing traits at the stem level

Three types of processing traits were analyzed. Digestibility-related traits were first considered as they constitute the primary targets of forage sorghum breeding programs. These traits are expected to present positive correlations with the biomethane potential which constitutes the main target of this study. In addition, higher heating value (also called gross energy, GE) was characterized as it constitutes a good proxy to determine the relevance of the considered biomass to produce energy in combustion scenario (Van Meerbeek, Appels, Dewil, Calmeyn, et al., 2015). Processing traits of stem samples were estimated by NIRS using the same NIR system as for the biochemical composition. For the in vitro dry matter digestibility (IVDMD) and the gross energy (GE), the calibrations are based on whole aboveground biomass and stem samples that were analyzed using the following reference methods. In vitro dry matter digestibility (IVDMD) of stem samples was measured according to an enzymatic method with cellulase and pepsin (Aufrère et al., 2007). In addition, in vitro NDF digestibility (IVNDFD) was calculated from IVDMD as follows: IVNDFD = 100−(IVDMD−((100−MM)-NDF))/NDF. IVNDFD represents the potential degradation of fiber in ruminants.

Higher heating value (or gross energy: GE) of the stem samples was measured from complete combustion of the samples in a bomb calorimeter (IKA C2000, IKA-Werke GmbH).

To estimate biomethane potential (BMP), the FlashBMP NIRS calibration (Ondalys, France) was used. It is based on more than 600 substrates including agro-industrial waste, green waste, energy crops, municipal solid waste, sludge, and digestate samples leading to build a robust and accurate model following the method described by Lesteur et al., (2011). The FlashBMP value is predicted in $NmLCH4g^{-1}$. VS and was converted in $NmLCH4g^{-1}$.DM expressed in normal conditions (0°C, 1.013 bar) and per gram of DM ($NmLCH4g^{-1}$) following the formula: BMP_DM = BMP_VS*(DM-MM)/DM where VS is the volatile solid content (g/g raw matter), DM the dry matter, and MM the mineral matter (in %DM). Unless explicitly specified the BMP expressed according to the dry matter (BMP_DM) will be considered in the following sections of this work (using the BMP abbreviation). NIR spectra were acquired on the NIR system 6500 spectrometer (FOSS NirSystem, Laurel, MD, USA) and transformed according to the method described by Chauvergne et al., (2020) in order to be used as input of the FlashBMP NIRS calibration model.

Accuracy of prediction models for the processing traits including their R^2, SEC (standard error of calibration), and SECV (standard error of cross-validation) are provided in Table S3.

2.5 | Data analysis

2.5.1 | Three panels of genotypes

Three panels of genotypes (Table S1) were considered in order to take advantage of the network of trials that had been established. A set of 21 genotypes (Panel21) available in at least three different trials was first considered in order to aggregate the three types of variables (biochemical,

histological, and processing related traits). A second set of 29 genotypes (Panel29) corresponding to the whole set of genotypes analyzed at the histological level (but also at the biochemical and processing levels) was considered to explore the global diversity available for this type of traits. Finally, the complete dataset (Panel57) was considered in order to analyze the relationships between the stem biochemical composition and the processing related traits on the largest panel available. The raw phenotypic datasets are provided in Table S4 (biochemical and processing traits) and Table S5 (histological traits).

2.5.2 | Variance components and broad sense heritability estimations

All the statistical analyses and graphics were performed using the R software (R Core Team, 2018). The same mixed model was used for the different datasets, specificities arose for the broad sense heritability calculations depending on the considered traits as the numbers of replications per genotype per site were not always the same (Table S3 and S4).

The linear mixed model considered was the following

$$Y_{ijk} = \mu + G_i + E_j + GE_{ij} + e_{ijk}$$

With Y_{ijk} corresponding to the phenotypic value of the k replicate of the genotype i on the experimental trial j with G_i corresponding to the random effect of the genotype i, E_j corresponding to the fixed effect of the experimental trial j (each experiment corresponding to one specific environment: 1 site for 1 year), GE_{ij} corresponding to the random interaction term between the genotypic effect i and experimental trial effect j, and e_{ijk} corresponding to the random error term. These analyses were performed with the lme4 R package and the best linear unbiased predictors (blup) of each genotype effect were extracted using the ranef function.

According to the variance components estimates of these models, broad sense heritability (h^2_{bs}) was calculated as $\sigma^2_g/(\sigma^2_g + \sigma^2_{ge}/e + \sigma^2_r/(e.r))$ with σ^2_g corresponding to the genetic variance, σ^2_{ge} corresponding to the variance of genotype × experimental trial interactions, σ^2_r corresponding to the residual variance, e corresponding to the number of experimental sites, and r corresponding to the number of replicates within sites. The number of replicates within site was dependent on the considered traits (five in average for histological data and one in average for biochemical and biomethane-related traits).

Blup values extracted from the mixed models obtained from Panel29 and Panel57 were used to explore the properties of the five genotypes harboring the lowest and highest values for the four processing traits considered. The low and high groups of each processing trait (five low and five high genotypes in each group) were compared for their histological (Panel29) and biochemical traits (Panel 29 and 57) through one factor analyses of variance considering a fixed group effect. In addition, the response of each group for the three other processing traits was also analyzed. To illustrate the properties of the low and high groups, radar charts based on the mean values of each group were built using the radarchart function from fmsb package.

2.5.3 | Multivariate analyses

Three types of correlations were calculated. Firstly, correlations between the phenotypic values obtained for a given trait in the different trials ($r_{TraitEi\text{-}TraitEj}$) were calculated to estimate the stability of the ranking of the genotypes between trials. Secondly, correlations between different traits in a given trial ($r_{Trait1Ei\text{-}Trait2Ei}$) were calculated for the different trials to evaluate the stability of correlations over trials. Thirdly, correlations between genotypic values extracted from the mixed model presented earlier were calculated. All correlation analyses were performed with the rcorr function of the Hmisc package and a critical value α of 0.05 was used for testing significance of these correlations.

Analysis of the effects of the midrib color (provided in Table S1) used here as proxy of the Dry gene alleles (Xia et al., 2018, only the white and green midribs were considered in this context) on the different traits was also performed by one factor ANOVA analysis.

Clustering analyses were also performed to better explore the behavior of the different genotypes using the hclust function of R stats package. Blup values of all the variables listed in Table 1 with the exceptions of CF and ADF (as CF is highly correlated to NDF and ADF is further divided in ADL and cellulose content) were considered to perform these clustering exercises.

Finally, stepwise regression analyses were performed in order to identify the most parsimonious combinations of traits able to explain the genetic variability (i.e., of blup values) observed for the four processing related traits. The R caret package was used, taking advantage of the train function. Briefly for each processing trait, linear regressions with stepwise selection were performed and the best models for each size of explanatory variable sets (from 1 to n-1, with n being the total number of explanatory variables) were tested. For each optimal set of different sizes, 10-fold cross-validation was used to estimate their average prediction error (RMSE) and the model harboring the lower RMSE was selected. According to the limits of the stepwise regression strategy used (that does not consider the significance of the effects of the different variables in the model) and our objective to understand the variability of the processing trait (and not to predict them),

TABLE 1 Phenotypic variability in the different experimental trials

		MPL2012 ($nG_b = 27$, $nG_h = 27$)[a]					MPL2013 ($nG_b = 30$, $nG_h = 18$)[a]					MPL2014 ($nG_b = 23$, $nG_h = 15$)[a]					MDN2013 ($nG_b = 23$)[a]					RIV2013 ($nG_b = 27$)[a]				
Trait type	**Trait**	**nS[b]**	**mean**	**min**	**max**	**PCV(%)**	**nS[b]**	**mean**	**min**	**max**	**PCV(%)**	**nS[b]**	**mean**	**min**	**max**	**PCV(%)**	**nS[b]**	**mean**	**min**	**max**	**PCV(%)**	**nS[b]**	**mean**	**min**	**max**	**PCV(%)**
Stem Dry matter composition	MM	49	5.29	2.03	9.90	37.21	30	5.82	2.87	10.87	34.79	23	6.79	3.31	11.21	34.07	75	3.21	−1.02	9.62	72.28	27	5.03	1.98	13.10	47.38
	CP	49	5.22	2.45	10.25	30.87	30	4.89	2.57	10.69	37.27	23	3.65	1.53	6.48	34.97	75	3.81	1.85	6.98	33.73	27	2.61	0.94	7.48	48.64
	SS	49	18.39	5.93	32.76	37.13	30	22.86	3.80	37.35	42.14	23	15.57	3.00	40.06	63.36	75	21.60	2.25	41.85	43.76	27	27.89	4.92	47.13	42.56
	CF	49	32.89	23.41	42.98	15.27	30	30.26	23.60	41.16	16.69	23	35.50	24.73	42.81	15.56	75	34.97	19.08	48.44	19.74	27	33.13	23.34	48.91	19.45
	NDF	49	61.98	47.34	74.97	12.07	30	56.98	44.08	75.74	15.33	23	62.20	41.54	75.02	15.94	75	64.17	42.90	85.59	16.36	27	58.34	41.91	82.28	17.25
Stem Fiber composition	ADF	49	35.23	24.10	47.38	16.90	30	32.74	23.93	45.13	18.18	23	37.28	25.35	46.69	17.75	75	37.99	18.46	55.06	22.01	27	35.20	24.22	53.22	20.00
	CVS	49	30.49	21.97	40.83	15.74	30	28.64	21.53	39.54	17.59	23	32.37	22.19	39.59	16.40	75	32.37	15.21	46.25	21.88	27	31.10	21.51	45.51	18.38
	HEMI	49	26.75	22.25	31.08	8.96	30	24.24	17.73	30.69	13.84	23	24.91	15.89	32.47	17.68	75	26.18	16.71	34.54	14.89	27	23.14	17.07	29.06	14.54
	ADL	49	4.74	2.10	7.63	29.44	30	4.11	1.50	6.20	28.44	23	4.91	2.09	8.07	38.49	75	5.61	1.34	9.71	31.03	27	4.10	1.46	7.71	37.27
	CVS_in_NDF	49	49.01	42.44	54.46	5.33	30	50.14	44.98	54.40	4.49	23	52.05	46.05	54.02	3.43	75	50.07	35.45	57.01	8.75	27	53.24	51.32	55.31	2.12
	HEMI_in_NDF	49	43.45	36.61	53.61	8.37	30	42.71	37.31	48.80	7.08	23	40.10	35.11	49.39	9.52	75	41.24	29.72	56.97	13.27	27	39.87	35.32	44.17	5.86
	ADL_in_NDF	49	7.53	3.95	10.97	22.28	30	7.14	3.20	9.41	21.50	23	7.85	2.97	11.37	31.24	75	8.70	2.32	13.61	24.15	27	6.89	2.70	9.53	24.36
Stem processing properties	IVDMD	49	47.21	29.79	62.35	18.25	30	52.87	37.96	66.66	15.83	23	43.42	29.93	62.24	22.60	75	42.72	20.17	61.34	24.80	27	48.31	22.61	62.64	22.78
	IVNDFD	49	19.85	8.63	36.92	32.84	30	23.14	7.78	47.84	37.97	23	12.60	1.73	29.54	67.71	75	14.07	1.42	37.39	55.19	27	18.10	8.13	39.74	44.26
	GE	49	1766.32	1670.00	1828.50	2.16	30	1759.40	1679.00	1813.00	1.71	23	1756.83	1672.00	1847.00	2.77	75	1781.57	1649.00	1872.00	2.40	27	1728.00	1585.00	1809.00	2.86
	BMP	49	242.10	203.00	280.00	8.41	30	263.70	224.00	297.00	8.13	23	228.78	192.00	301.00	12.35	75	252.84	204.00	302.00	9.31	27	270.41	200.00	342.00	14.66
Internode anatomy	percZ1	158	16.39	10.16	26.22	17.57	100	15.69	8.55	25.80	23.15	54	15.70	11.62	26.55	19.50										
	percSclZ1	157	54.02	18.69	76.28	22.59	100	28.91	11.57	42.20	22.96	54	43.12	20.99	62.82	26.56										
	percbluZ2	158	34.66	0.00	90.35	76.87	100	26.33	0.22	81.49	72.10	54	26.43	0.01	86.56	99.66										
	nbVBZ2	157	171.56	92.00	310.00	29.73	100	151.02	76.00	254.00	27.39	54	124.81	68.00	201.00	26.36										
	densVBZ2	157	1.15	0.68	1.77	21.04	100	1.30	0.67	2.82	28.27	54	1.33	0.55	2.56	30.33										

[a]nGb corresponds to the number of genotypes considered for the biochemical and BMP analyses. nGh corresponds to the number of genotypes considered for the histological analyses.

[b]nS corresponds to the number of individual samples analyzed for each trait.

the variables included in the most parsimonious models identified were also characterized according to the significance of their effects on the processing traits. For each processing trait, the stepwise regression analyses were performed on Panel29 (including biochemical and histological variables) and on Panel57 (including only biochemical variables).

3 | RESULTS

3.1 | Phenotypic variabilities observed between the different experimental trials

A total of 57 genotypes were analyzed for biochemical and processing traits of the stem in five experimental trials. For a given trait, the levels of phenotypic variability (PCV) observed in the different experiments were consistent. However, different patterns of phenotypic diversity were observed among the traits (Table 1). Among the dry matter composition traits, CF and NDF exhibited the lowest phenotypic diversities (PCV around 15%). Regarding fiber composition-related traits, the highest phenotypic variabilities were observed for the lignin contents (ADL and ADL_in_NDF) and the lowest ones for the hemicellulose contents (HEMI and HEMI_in_NDF). For the processing properties, highly divergent patterns of phenotypic variability were observed. BMP presented an average PCV across sites of 10% whereas digestibility-related traits harbored two (IVDMD) to five (IVNDFD) times higher variability levels. GE exhibited the lowest variability observed overall.

For the histological traits, all the genotypes presented a similar internode organization plan composed of two main anatomical zones (Figure 1). The outer zone Z1 is characterized by a lignified epidermis and vascular bundles (VB) surrounded by a sclerenchyma with thick lignified cell wall. The inner zone Z2 is mainly composed of parenchyma cells and VB. Phenotypic variabilities ranging from 20% to 30% in average were observed with the exception of percbluZ2 that exhibited consistently extremely large phenotypic coefficient of variations across sites (from 72% to 99%).

Considering all the biochemical and processing traits, the average correlation observed between environments for a given trait was 0.69, with an average *P* value (*P*) of 0.036 across all the traits (Figure S2, Table S6). Considering specifically BMP, phenotypic correlations between trials ranged from 0.50 to 0.79 with all but one *P* being significant at the 0.05 critical threshold.

For histological traits, the average phenotypic correlations between sites for a given trait ranged from 0.4 for percSclZ1 (average *P* of 0.36) to 0.82 for nbVBZ2 (average *P* of 0.002) (Table S7). Apart from percSclZ1 for which the results from the MPL_2014 experiment appeared atypical, the phenotypic values observed across the experiments were highly consistent (Figure 2).

3.2 | Broad sense heritability and genetic coefficients of variation

Broad sense heritability was computed for the three panels of 21, 29, and 57 genotypes (Table 2). Heritability estimates were consistent across the different panels. Heritability over 0.85 was observed for most of the traits with CVS_in_NDF exhibiting the lowest values (from 0.66 to 0.79) and IVNDFD exhibiting the highest ones (from 0.94 to 0.96). Large differences were observed between traits for the levels of genetic variance.

For histological traits, heritability ranging from 0.42 to 0.94 was observed, these values being consistent between the two panels of 21 and 29 genotypes. PercZ1 presented a high broad sense heritability accompanied by a moderate level of genetic variability (13%). The lowest heritability was observed for percSclZ1 (0.42 and 0.48) in accordance with the atypical result obtained in MPL_2014 trial. PercbluZ2 presented the highest level of genetic variability (53–58%) across all the considered traits associated with a high broad sense heritability (0.76–0.77). Finally, nbVBZ2 exhibited a high heritability associated with a large genetic variance (h^2_{bs} = 0.88–0.94 and GCV = 22.6–27.1%) whereas densVBZ2 presented lower estimates (h^2_{bs} = 0.65–0.66 and GCV = 14.9–16.3%).

3.3 | Genetic correlations between traits

According to the genetic values (blup) of each genotype, genetic correlations between traits were estimated. As a first step, correlations between processing traits were analyzed (Figure 3a). A significant positive correlation was observed between BMP and IVDMD (r_g = 0.75, $p < 0.001$) whereas a nonsignificant correlation was observed between the BMP and GE (r_g = −0.01, p = 0.9). As a second step, genetic correlations between processing and biochemical traits were explored (Figure 3b). A highly significant positive genetic correlation was observed between BMP and SS (r_g = 0.9, $p < 0.001$), all the germplasm types following exactly the same pattern (Figure 3c). Accordingly, highly negative correlations were observed between BMP and CF (r_g = −0.76, $p < 0.001$) and NDF (r_g = −0.85, $p < 0.001$). Overall, correlations observed between BMP and the stem biochemical components in sorghum are consistent with the ones reported for maize on whole aboveground biomass (Rath et al., 2013). It is also interesting to mention

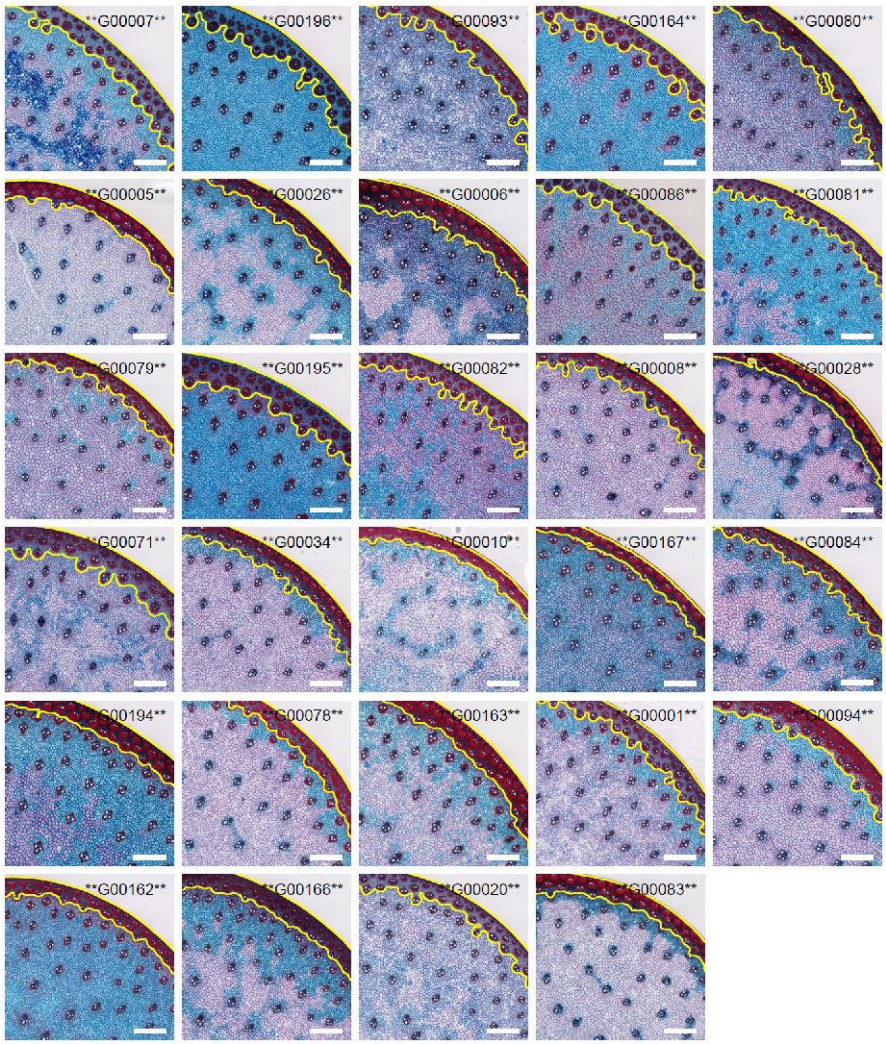

FIGURE 1 Histological cross section stained by Fasga of the internodes of the stem of the main shoot of the 29 genotypes characterized on the different sites. The yellow line delimits the border between zone 1 (Z1, external zone) and zone 2 (Z2, internal zone) of the internode. Genotypes are ranked according to their percentage of sclerenchyma in the outer Z1 region (percSclZ1). The genotype G00007 (IS26731) presented the lowest percentage whereas G00083 (IS30417) presented the highest value. The variance component analysis confirmed that these differences are highly dependent of the genotype, heritability ranging most of the time between 0.6 and 0.8 being obtained for the different histological traits. The scale bars on the bottom right side of the internode sections correspond to 1000 μm

that none of the proportions of cellulose, hemicelluloses, or lignins of the NDF were correlated to BMP. IVDMD globally presented the same pattern of correlations as BMP with a higher impact of the cell wall content compared to the soluble sugars and significant impacts of the relative contents of the different cell wall components (CVS_in_NDF: $r_g = -0.55$, $p < 0.001$, HEMI_in_NDF: $r_g = 0.68$, $p < 0.001$). The highest correlations detected for GE involved the lignin-related traits (ADL: $r_g = 0.81$, $p < 0.001$ and ADL_in_NDF: $r_g = 0.84$, $p < 0.001$) and MM ($r_g = -0.83$, $p < 0.001$).

In order to reach a better understanding of the traits contributing to the genetic variabilities of the processing traits, residues of the linear models involving the main biomass components (Table S8) affecting these traits were also analyzed (Figure 3a). For BMP, analysis of the residues of SS content revealed significant correlations with the lignin content (ADL and ADL_in_NDF) and CP (Figure 3b). Slightly different correlations (different slopes) between the BMP residues and these variables were observed in the breeding material and landraces compartments (Figure 3c). The same results with an additional positive correlation of CVS_in_NDF were observed for IVDMD adjusted to ADF.

As a third step, correlations involving histological, biochemical, and processing traits were also explored (Figure 4, Table S8). Among histological traits, a negative correlation ($r_g = -0.38$, $p = 0.045$) was detected between percSclZ1 and percbluZ2. In addition, a significant negative correlation was observed between percZ1 and nbVBZ2 ($r_g = -0.47$, $p = 0.01$). Regarding the genetic relationships of histological and biochemical traits, highly positive correlations were

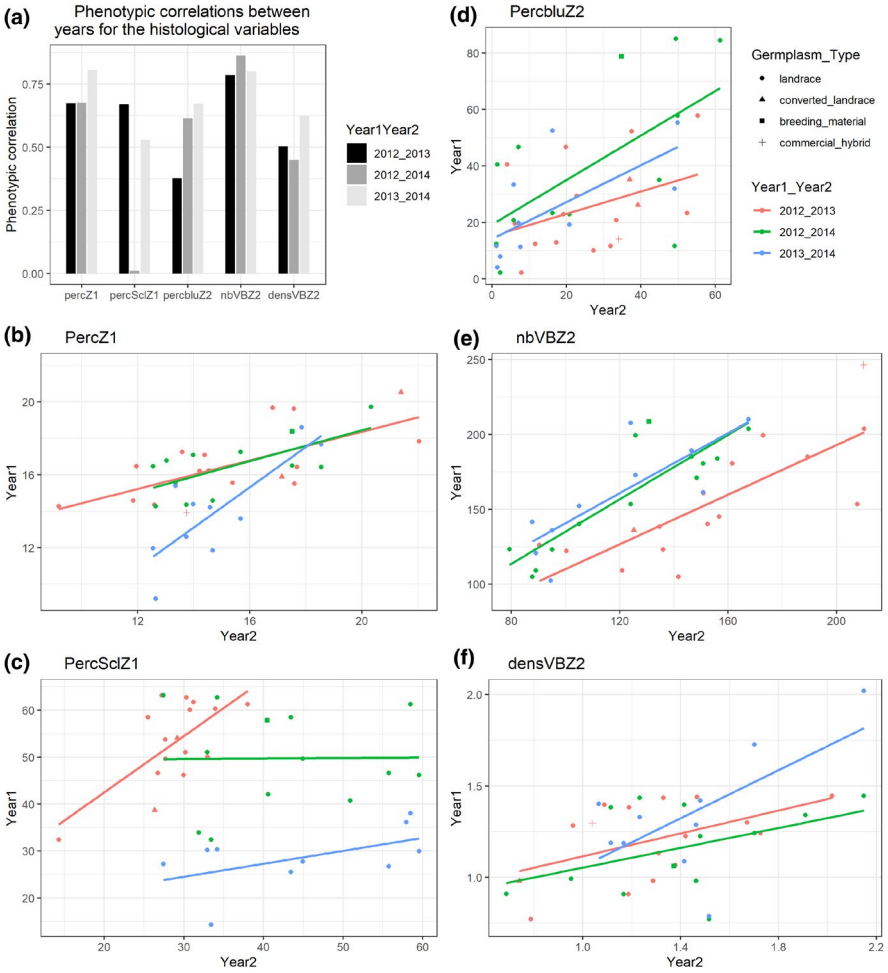

FIGURE 2 Phenotypic correlations between years for the histological variables measured on the internodes (see also Table S7 for details). (a) Comparisons of the phenotypic correlations observed between years for the different histological variables. (b), (c), (d), (e), (f): Variabilities observed between the years for the different histological variables. Germplasm types are indicated by different symbols and the combinations of experiments considered are indicated with different colors. Regression lines for each combination of experiments are also provided

observed between perSclZ1 and the less digestible fractions of the biomass (CF: $r_g = 0.62$; $p < 0.001$, NDF: $r_g = 0.55$, $p < 0.001$). Opposite trends were observed for percbluZ2, that presented highly negative correlations with these same traits and especially with the lignin content of the fibers (ADL_in_NDF: $r_g = -0.74$, $p < 0.001$). DensVBZ2 presented positive correlations with ADL ($r_g = 0.44$, $p = 0.015$) and ADL_in_NDF ($r_g = 0.48$, $p = 0.008$).

Significant correlations were also detected between the histological traits and processing related traits. Negative correlations were observed between percSlcZ1, IVDMD ($r_g = -0.58$, $p < 0.001$), and IVNDFD ($r_g = -0.51$, $p < 0.005$) whereas positive ones were observed between percbluZ2 ($r_g > 0.6$, $p < 0.0005$), nbVBZ2 ($r_g > 0.27$ with a significant P for IVDMD and nonsignificant P for IVNDFD), and these two processing traits. For GE, an opposite correlation pattern was observed with the histological traits mentioned above in comparison to the digestibility-related traits.

3.4 | Hierarchical clustering analyses

The hierarchical clustering analysis based on the 29 genotypes analyzed at the histological, biochemical, and processing levels (Figure 4) revealed two main groups of traits "T29_1" and "T29_2". "T29_2" group includes traits positively correlated to biomass and cell wall digestibility-related traits (IVDMD, BMP, IVNDFD). They correspond to biochemical traits like SS, HEMI_in_NDF, and CP. In addition, histological traits like nbVBZ2 and percbluZ2 also correlate positively with the degradability-related traits. At the opposite, the "T29_1" group includes traits negatively correlated to the degradability of the biomass and of the cell walls such as the lignocellulosic components (NDF, CF, ADF, CEL, ADL). At the histological level, percSclZ1 and densVBZ2 also correlate negatively to the degradability-related traits. The hierarchical clustering

TABLE 2 Broad sense heritability and genetic variance estimates over the different panels (21, 29, and 57 genotypes)

		Panel 21 genotypes		Panel 29 genotypes		Panel 57 genotypes	
Trait type	**Trait**	**h^2_{bs}**	**GCV(%)**	**h^2_{bs}**	**GCV(%)**	**h^2_{bs}**	**GCV(%)**
Stem Dry matter composition	MM	0.89	31.78	0.90	31.45	0.93	36.46
	CP	0.82	23.84	0.88	29.31	0.86	28.08
	SS	0.88	37.97	0.88	34.34	0.88	33.66
	CF	0.92	14.84	0.92	14.73	0.91	14.44
	NDF	0.90	12.25	0.90	12.27	0.90	12.09
Stem Fiber composition	ADF	0.90	15.51	0.90	15.92	0.89	15.26
	CVS	0.90	14.71	0.90	14.58	0.88	14.38
	HEMI	0.84	9.85	0.85	9.79	0.85	10.09
	ADL	0.91	25.20	0.93	30.02	0.91	27.54
	CVS_in_NDF	0.74	3.37	0.79	3.49	0.66	3.15
	HEMI_in_NDF	0.83	6.83	0.87	7.73	0.81	6.71
	ADL_in_NDF	0.89	17.46	0.93	22.50	0.91	21.43
Stem processing properties	IVDMD	0.93	18.84	0.94	18.61	0.93	16.59
	IVNDFD	0.94	37.32	0.95	38.49	0.96	39.92
	GE	0.87	1.51	0.91	1.81	0.93	2.07
	BMP	0.87	8.72	0.87	8.06	0.86	7.96
Internode anatomy	percZ1	0.79	13.06	0.81	12.93		
	percSclZ1	0.42	11.29	0.48	11.14		
	percbluZ2	0.76	58.43	0.77	53.93		
	nbVBZ2	0.88	22.57	0.94	27.05		
	densVBZ2	0.65	16.28	0.66	14.89		

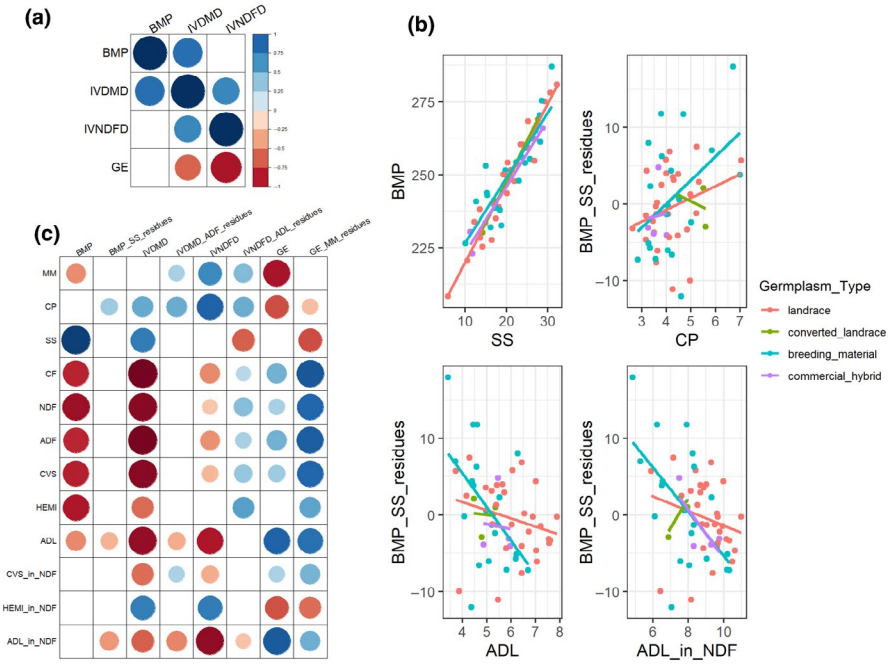

FIGURE 3 Genetic correlations between processing related traits and stem composition biochemical traits. (a) Correlations between processing traits, (b) Correlations between processing and biochemical traits only the correlations significant at the 0.05 critical threshold are provided (see also Table S8 for more details). (c) Correlations between BMP and its main biochemical contributors

analysis also allowed the detection of four main groups of genotypes (G29_A to G29_D, Table S9). G29_A and G29_B groups are characterized by low biomass and cell wall degradabilities associated with low BMP (Figure 4c). Whereas G29_C and G29_D harbored the same high levels of IVDMD, they differed significantly regarding BMP and IVNDFD. G29_C is characterized by the highest IVNDFD likely in relation with its high frequency of genotypes harboring brown midrib alleles (G00195, G00086, and G00196) that translate in the lowest ADL_in_NDF (Figure S3) while G29_D presents the highest BMP. The superiority of G29_D for BMP can be putatively linked to its high level of soluble sugar content (Figure S3). The G29_B group harbors the lowest degradability (IVDMD and IVNDFD) and it is enriched in bicolor and guinea genotypes.

A hierarchical clustering analysis was also performed based on biochemical and processing traits obtained on Panel57. This analysis allowed the detection of three main genotype clusters that can be further subdivided in six subclusters (Figure S4, Table S10). A large similarity of the two hierarchical clustering exercises (based on Panel29 and Panel57) was revealed. Almost all the genotypes included in the G29_C and G29_D clusters were included in the G57_C cluster, these three clusters being characterized by high BMP and biomass digestibilities. In contrast, almost all the genotypes from the G29_A and G29_B clusters were allocated to the G57_A and G57_B clusters, these four clusters harboring low biomass digestibility and BMP. The largest diversity covered in Panel57 also allowed to refine some patterns. Consistently with the clustering exercise performed on Panel29, only one bmr genotype (G00196) was included in the high BMP cluster of Panel57 (G57_C) revealing that low lignin content is not strictly required to maximize BMP. In addition, the low BMP cluster of Panel57 (G57_A) is highly enriched in breeding materials and commercial hybrids whereas the high BMP cluster (G57_C) benefited of a larger contribution of the landraces (50% in comparison to 27% in G57_A). The properties of the clusters identified on Panel57 are described in Figure S5 for the global stem dry matter-related traits and Figure S6 for the cell wall-related traits.

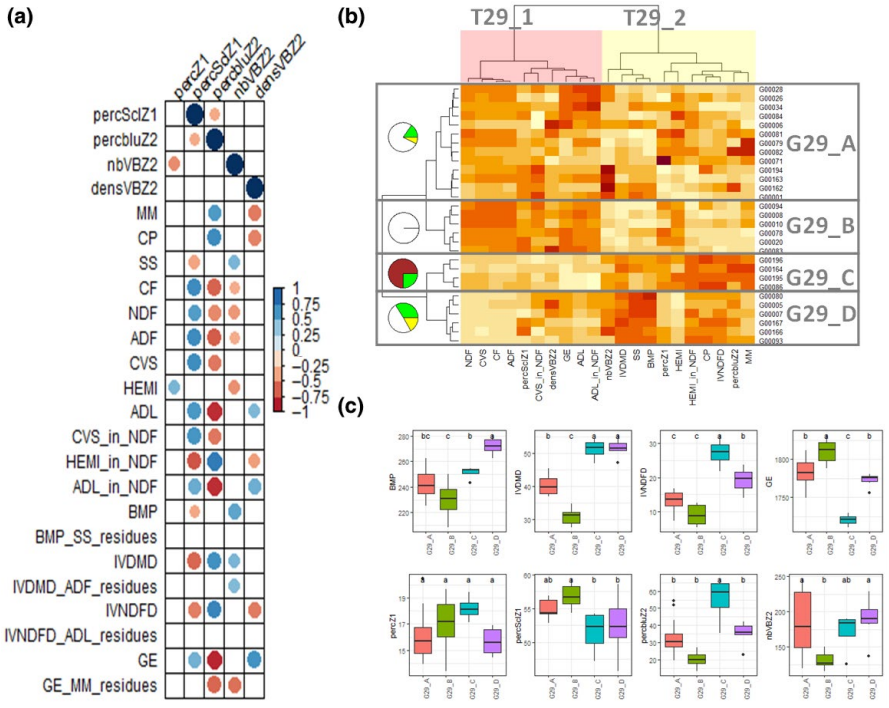

FIGURE 4 Genetic relationships between the stem histological, biochemical and processing traits. A) Genetic correlations between the processing traits and the stem biomass composition related traits, only the correlations significant at the 0.05 critical threshold are provided. B) Hierarchical clustering analysis of the histological, biochemical and processing related traits for the 29 genotypes analyzed jointly for these three types of traits. Red cells indicate low values whereas yellow ones correspond to high values. Pie charts on the left side indicate the proportions of accessions in each group harboring the different midrib colors (green stands for green midrib, white stands for white midrib, yellow stands for yellow midrib and brown stands for brown midrib (bmr)). C) Variability of the industrial related traits (top line) and of the histological traits between the genotype's clusters identified. Different letters over the boxplots indicate that the clusters significantly differ in relation with the considered trait ($p<0.05$)

3.5 | Characterizing genotypes harboring extreme values for processing traits

With the aim to contribute to the identification of stem ideotypes maximizing the performances for the four processing traits considered, genotypes harboring the lowest and highest blup values for these traits were identified (Table S9 and Table S10). Differences between the two groups (five genotypes were considered for each) were characterized through one factor analysis of variance. These analyses were performed on Panel29 taking advantage of biochemical and histological traits (Figure 5 and Figure S7) and on Panel57 considering exclusively biochemical traits (Figures S8 and S9). These analyses allowed to highlight several differences in terms of behavior for BMP and IVDMD extreme groups. Firstly, a larger effect on SS was detected for BMP compared to IVDMD (Figure 5 and Figure S8). Secondly, all the relative proportions of the fiber components (CVS_in_NDF, HEMI_in_NDF and ADL_in_NDF) were significantly different between the extreme groups for IVDMD, but only CVS_in_NDF was marginally significant between the two BMP groups. Thirdly, IVDMD and BMP extreme groups differed in relation to their histological related traits. For IVDMD, significant differences were observed for percSclZ1, percbluZ2, and nbVBZ2 whereas only this last variable was significantly different between the extreme groups of BMP.

3.6 | Multiple linear regression analyses with stepwise selection

In order to reach a better understanding of the biochemical and histological traits impacting processing traits, multiple linear regression analyses with stepwise selection were performed for the 29 genotypes and 57 genotypes panels (Table 3). Compared with the approach developed in the previous paragraph 3.5, this strategy takes advantage of the whole set of genotypes analyzed and hence of the global genetic diversity analyzed. These analyses aimed at identifying the main biochemical and

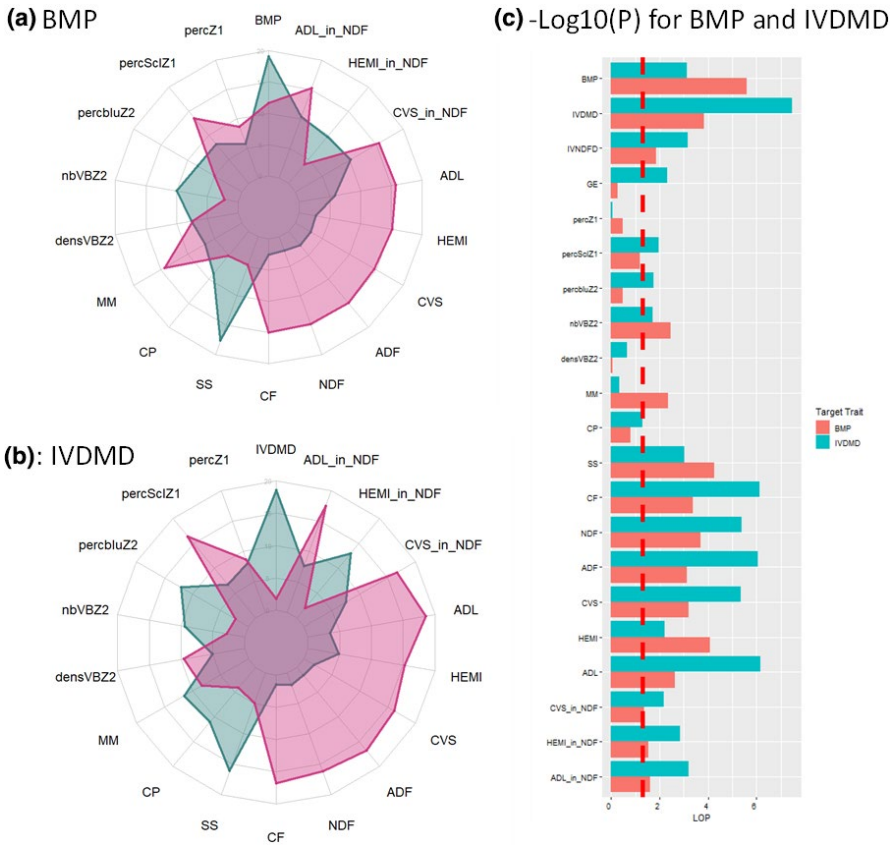

FIGURE 5 Comparisons of the top5 and low5 genotypes for BPM and IVDMD based on Panel29 regarding their processing, biochemical, and histological properties. Radar plots of the biochemical and histological traits are provided for both processing traits, (a): BMP, (b): IVDMD. The green areas indicate the mean values of the top5 genotypes whereas the pink ones indicate the mean values of the low5 genotypes. (c) Log10(pvalues) of the group effect (low5 vs. top5) are indicated on the right panel. The red bars correspond to the Log10(Pvalues) of the group effect for BMP and the green ones correspond to the Log10(Pvalues) of IVDMD. The dashed red line indicates the critical significance threshold $p = 0.05$

TABLE 3 Identification of the traits contributing to the variability of the processing target traits through stepwise regression analyses. As stepwise regression analyses are based on AIC optimizations and as the significance of the effects of the traits are not considered in these analyses, significance of the effects of the different traits in the processing targets have been analyzed through classical linear models

Trait	Considered traits[a]	Panel	Component traits selected through Stepwise regression[b]	$RMSE_{lstep}$[c]	r^2_{lstep}[d]	$Coefficients_{lm}$[e]	P_{lm}[f]
BMP	Biochemistry and Histology	29	MM, SS, ADL_in_NDF	4.158	0.939	intercept: 266.320, MM: −4.242, SS: 2.021, ADL_in_NDF: −5.057	intercept: $p < 0.001$, MM: $p < 0.001$, SS: $p < 0.001$, ADL_in_NDF: $p < 0.001$
BMP	Biochemistry	57	MM, ADL, SS, CVS_in_NDF	4.362	0.957	intercept: 167.523, MM: −4.187, ADL: −8.476, SS: 1.458, CVS_in_NDF: 2.275840	intercept: 167.523105, MM: $p < 0.001$, ADL: $p < 0.001$, SS: $p < 0.001$, CVS_in_NDF: $p < 0.001$
IVDMD	Biochemistry and Histology	29	CP, NDF, ADL	1.085	0.996	intercept: 97.306, CP: 1.104, NDF: −0.7134, ADL: −2.257	intercept: $p < 0.001$, CP: $p < 0.01$, NDF: $p < 0.001$, ADL: $p < 0.001$
IVDMD	Biochemistry	57	MM, CP, NDF, HEMI_in_NDF, ADL^{ns}, SS^{ns}, $HEMI^{ns}$, $ADL\_in\_NDF^{ns}$	1.293	0.968	intercept: 154.690, MM: −0.580, CP: 1.146, NDF: −1.382, ADL: −2.222, SS: −0.171, HEMI: 1.407, HEMI_in_NDF: −1.004, ADL_in_NDF: −0.546	intercept: $p < 0.001$, MM: $p = 0.024$, CP: $p = 0.001$, NDF: $p < 0.001$, ADL: $p = 0.143$, SS: $p = 0.324$, HEMI: $p = 0.069$, HEMI_in_NDF: $p = 0.022$, ADL_in_NDF: $p = 0.552$
IVNDFD	Biochemistry and Histology	29	percbluZ2, CP, ADL, SS	1.780	0.960	intercept: 42.447, percbluZ2: −0.066, CP: 1.708, ADL: −4.697, SS: −0.246	intercept: $p < 0.001$, percbluZ2: $p = 0.0418$, CP: $p = 0.001$, ADL: $p < 0.001$, SS: $p < 0.001$
IVNDFD	Biochemistry	57	CP, $HEMI^{ns}$, ADL_in_NDF	2.531	0.782	intercept: 36.205, CP: 2.548, HEMI: −0.158, ADL_in_NDF: −3.129	intercept: 36.204546, CP: $p < 0.001$, HEMI: $p = 0.0396$, ADL_in_NDF: $p < 0.001$
GE	Biochemistry and Histology	29	percSclZ1, MM, ADL, HEMI	7.587	0.952	intercept: 1755.821, percSclz1: −1.233, MM: −13.128, ADL: 12.947, HEMI: 2.241	intercept: $p < 0.001$, percSclz1: $p = 0.016$, MM: $p < 0.001$, ADL: $p < 0.001$, HEMI: $p = 0.005$
GE	Biochemistry	57	MM, ADL	9.047	0.945	intercept: 1721.046, MM: −10.561, ADL: 15.813	intercept: $p < 0.001$, MM: $p < 0.001$, ADL: $p < 0.001$
GE	Biochemistry	57	MM, ADL	9.047	0.945	intercept: 1721.046, MM: −10.561, ADL: 15.813	intercept: $p < 0.001$, MM: $p < 0.001$, ADL: $p < 0.001$

[a]For biochemical traits, CF and ADF have not been considered as CF is highly correlated to NDF and ADF is further divided in ADL and cellulose content.

[b]Traits for which nonsignificant effects have been detected in the restricted model containing only the traits identified through stepwise regression analyses are indicated with the ns superscript.

[c]Root Mean Square Error of the model identified using the linear stepwise regression analyses.

[d]R square of the model identified using the linear stepwise regression analyses.

[e]Effects of the traits belonging to the model, identified using linear stepwise regression analyses, obtained through a linear model.

[f]Significance of the effects of the traits involved in the model, identified using linear stepwise regression analyses, obtained through a linear model.

histological traits contributing to the variability of the processing targets considering their covariances. For BMP, analysis of Panel57 highlighted the major impacts of four biochemical related traits, namely, SS, ADL, MM, and CVS_in_NDF, with ADL and MM exhibiting the largest effects. Addition of histological related traits did not improve the prediction model. For IVDMD, the same pattern was observed, the best model involving exclusively biochemical traits with a much lower impact of SS. Results were slightly different for IVNDFD and GE for which better prediction models were obtained through the inclusion of histological related traits (percbluZ2 and percSclZ1 respectively).

4 | DISCUSSION

As underlined by Xu et al., (2019), improving plant biomass composition toward their use for biogas production presents several advantages compared to the optimization of biomass pretreatment. Indeed, this strategy does not require additional energy nor chemical inputs, it produces no toxic by-products and causes less pollution to the environment. With the aim to determine a sorghum stem ideotype maximizing methane production potential, the variability of this trait was explored over a panel of 57 genotypes including landraces, breeding material, and commercial hybrids. This analysis was focused on methane production potential per stem dry matter unit in order to allow an in-depth analysis of this yield component independently of the total dry matter production. Through this analysis, the explorations initiated by Mahmood and Honermeier (2012) (5 cultivars), Mahmood et al., (2013) (14 cultivars), Windpassinger et al., (2015) (13 cultivars), and Pasteris et al., (2021) (6 cultivars) on whole plant samples were extended to a larger set of sorghum genotypes and specifically targeted toward the stem compartment which represents 70–40% of the dry biomass yield for this category of sorghum cultivars. The genetic parameters of biomethane potential at the stem level were estimated in order to assess the selection ability for this trait. In addition, multivariate analyses were performed to identify the combination of traits that could maximize BMP. The discussion section will be articulated around three parts. Firstly, the genetic determinism of biomethane production will be discussed. Secondly, lessons based on the structure of the genetic variability (i.e., race, germplasm type effects) revealed for histological traits and the usefulness and challenges linked to this type of traits will be presented. Thirdly, biochemical, histological, and biomethane production results will be integrated toward the definition of a stem methane ideotype for sorghum and its comparison with ideotypes targeting animal feed and combustion.

4.1 | Biomethane potential can be improved through optimization of specific stem traits

The phenotypic variability observed for stem biomethane potential over the 57 genotypes analyzed (ranging from 192 to 342 $NmL_{CH4}.g_{DM}^{-1}$, corresponding to 205–355 $NmL_{CH4}.g_{VS}^{-1}$) is in accordance with the ones previously reported for the whole aboveground biomass that range from 232 to 427 $NmL_{CH4}.g_{VS}^{-1}$ (Mahmood & Honermeier, 2012; Mahmood et al., 2013; Pasteris et al., 2021; Sambusiti et al., 2013; Windpassinger et al., 2015). Consistently with the significant genotype effect reported in these studies, high broad sense heritability (ranging from 0.86 to 0.87) combined with moderate coefficients of genetic variation (8% in average) were observed at the stem level. According to these results, maximization of methane production potential based exclusively on the stem compartment, taking advantage of the genetic diversity available in *Sorghum bicolor ssp bicolor*, is a relevant option. Genotypes harboring the highest stem biomethane production per unit of dry matter include landraces that can provide additional relevant alleles to the breeding material. Breeding for biomethane potential will benefit of the high throughput phenotyping tools already available to directly characterize this processing trait (Chauvergne et al., 2020), but also as described in the two following sections, from the tools developed to characterize the stem properties.

Beside methane production potential, in vitro dry matter digestibility and cell wall digestibility variabilities were also analyzed. For these last two processing traits, broad sense heritability and phenotypic variabilities obtained are in accordance with the results reported by Trouche et al., (2014). Genetic correlation analyses revealed strong links between the stem dry matter digestibility and the stem methane production potential allowing the use of stem digestibility estimates to predict, as a rough proxy, the methane potential. However as indicated in the next sections, different ideotypes need to be targeted to maximize the gains for both traits.

High broad sense heritability was also observed for the higher heating value, but conversely to the methane potential and stem digestibility traits, this processing trait exhibited a limited genetic variability. Additional information is required from the thermochemical production routes (and more specifically combustion) to evaluate if the genetic variability available in sorghum for gross energy would be sufficient to allow genetic gains relevant for this type of second-generation bioenergy.

As a significant genetic variability exists for stem methane production potential, identification of the stem properties contributing to this trait will provide specific

strategies to optimize its selection. In order to reach a better understanding of the stem structure, its histological variability was analyzed.

4.2 | Genetic variability of histological traits

Moderate to high broad sense heritability associated with genetic coefficients of variation over 10% was observed for all the histological traits These results confirm the detection of significant genotype effects in previous studies performed by Perrier et al., (2017) and Luquet et al., (2019) on narrower panels of genotypes (2 and 8, respectively). Although histological analyses were only performed on one site over 3 years, questioning the existence of genotype by site interactions, the medium to high inter-year correlations observed combined with the weak effects of genotype by year and genotype by water availability treatments reported by Luquet et al., (2019, see their Table 5) suggest a relatively stable ranking of the genotypes across environmental conditions. Broad sense heritability observed for the outer Z1 region area roughly corresponds with the repeatability reported by Gomez et al., (2018) on sorghum for their "rind area" trait (0.72). It is also interesting to note the difference detected between the number of vascular bundles and their density in the Z2 inner region, with the number of vascular bundles exhibiting a higher broad sense heritability. This observation could be linked to the early determination of the number of vascular bundles which would be mainly under genetic control whereas the density depends on internode diameter growth which is impacted by environmental conditions as observed by Perrier et al., (2017), Tsuchihashi and Goto (2005), and Salih et al., (1999). This observation is also consistent with Legland et al., (2017) and El Hage et al., (2018) on maize who observed only a significant genotype effect on the vascular bundle number whereas genotype and water treatment effects were observed for the vascular bundle density.

The moderate negative correlation observed between the percentage of red sclerenchyma tissue in Z1 and the percentage of blue parenchyma tissue in Z2 suggests only a partial similar genetic control of these two traits. This result is in accordance with the differential responses observed for the lignin deposition in these two internode regions in different environmental conditions (Luquet et al., 2018; Perrier et al., 2017). This observation also fits with the negative, although nonsignificant, correlation detected between the proportion of blue parenchyma tissue in the inner internode Z2 region and the proportion of red tissue in the rind (Z1 outer internode region) reported by El Hage et al., (2018) in maize.

Significant correlations between histological and biochemical traits were detected. As expected, the percentage of sclerenchyma in the outer region positively correlates with the lignin content of the biomass. The same type of correlation was observed in maize by El Hage et al., (2018) with a positive correlation (0.74) between the red rind and the Klason lignin content. Conversely, a positive correlation was observed between the percentage of blue staining in the inner region and the hemicellulose content of the cell wall. These relationships between histological and biochemical traits were expected as both are linked to the concentrations and distributions of the main cell wall components. Nevertheless, the interest of histological related traits should not be limited to their ability to anticipate biochemical composition. Indeed, if the histology-related traits used in these analyses are limited by their 2D character, they provide a spatial information that is complementary with the 3D "destructured and blind" information provided by biochemical analyses. They provide an access to the spatial distribution of the cell wall structural macromolecules that is likely to be key to disentangle the factors affecting processing traits based on the stem compartment.

Although significant genetic variabilities have been detected for the histological traits ensuring the ability to manipulate them at the genetic level, it is also, from a breeder's perspective, essential to reach a clear vision of the structure of this diversity. Hierarchical clustering and variance components analyses revealed that the bicolor and guinea genotypes are characterized by low number of vascular bundles and low area of blue in the inner region of the internodes. They also present the highest percentages of sclerenchyma in the outer region of the internode. Although a large histochemical variability is observed regarding the durra and caudatum races, they encompass some of the genotypes harboring the highest number of vascular bundles and higher area of blue in the inner region of the internodes. These results also indicate that sorghum landraces have the potential to provide the breeding programs with relevant alleles depending on the end-product targeted as they carry histological properties that are not well distributed in the breeding materials. Nevertheless, if the histological pipeline established in this study offers the opportunity to develop medium throughput phenotyping suitable to identify donor parents, it is not well dimensioned to support the requirements of a breeding program in which thousands of candidate genotypes have to be evaluated. To achieve this throughput, simplification of the harvest, sample preparation (avoiding the cutting steps), and staining steps (avoiding the fixation step) combined with the use of deep learning algorithm already developed in ImageJ

(Arganda-Carreras et al., 2017; Gómez-de-Mariscal et al., 2019) constitute logical evolutions. The X-ray computed tomography pipeline developed by Gomez et al., (2018) that allows access to several stem anatomical parameters (rind area, pithiness, intensity (a proxy of stem dry weight density)) with a medium throughput constitutes a highly relevant complementary tool. Although X-ray tomography will probably not allow to access the proportions of tissues in the different internode sections, and will be difficult to mobilize in developing countries (where sorghum-based bioenergy production is also at the agenda and where control of sample water content can be challenging), the exploration of the correlations between the traits accessible by this method and the Fasga staining information achieved in the present study would be extremely interesting. A last aspect that merits to be raised regarding histological analyses is the consistency of the observations made in sorghum and maize not only regarding the genetic determinism of these traits but also their links with biochemical traits. These results highlight the benefits of comparative analyses of these two species for the sake of their specific breeding programs.

4.3 | Biomethane Potential (BMP) ideotype

As the stem largely contributes to the overall biomass yield for industrial and double purpose sorghum ideotypes that are targeted for energy production, there is a clear interest to accurately identify the biochemical and histological properties allowing to maximize energy yield. According to the present study, it appears, that although the stem biomethane potential significantly correlates with the stem in vitro matter digestibility ($r_g = 0.75$, $p < 0.001$), as also reported on whole aboveground biomass by Pasteris et al., (2021), specific strategies need to be developed to optimize genetic gains for these two traits. Indeed, different contributing traits were identified for these targets. Although genetic correlation, multiple regression, and hierarchical clustering analyses highlighted different contributions of the biochemical components to the BMP (as expected according to their different underlying hypotheses), they converged regarding the major impact of SS on this processing target. For IVDMD, SS appears to be less important than the concentrations of the cell wall components.

As a consequence, for BMP as for first-generation ethanol production based on stem soluble sugars (Guden et al., 2020), there is a higher priority to mobilize alleles maximizing the soluble sugar content of the stem in the elite BMP varieties than to manipulate the cell wall composition. Nevertheless, analysis of midrib color variability, which is a proxy of the dry gene alleles (green (juicy) vs. white (dry)) whose impact on sugar yield has been confirmed (in Xia et al., 2018 but also in the present study ($p < 0.012$)), in our panel, did not reveal a significant impact on the Biomethane potential ($p > 0.064$). This result suggests that although this major gene is probably important as it partially drives sugar content variability, it interacts with other histological and biochemical component to contribute to the BMP.

In addition, it is important to remind that genotypes carrying bmr alleles, that harbor extreme lignin content, are not the ones that present the highest methane production potential at the stem level. Taking into consideration these results, mid- and long- term optimization of genetic gains for BMP will clearly rely on joint breeding efforts for soluble sugars and cell wall components with the key roles of the lignin (negative impact) and of the cellulose contents (positive impact). Although our experimental design was not well suited to explore the links between lodging susceptibility and the biochemical, histological, and processing traits we analyzed, their clarifications are obviously of paramount importance for breeding programs. To be conclusive, these analyses will require the analyses of genotypes harboring the same plant sizes taking advantage of the methodologies developed recently by Gomez et al., (2018, 2017).

It is also interesting to mention the relative convergence between the results obtained in sorghum stems and maize whole aboveground biomass in which the impacts of the water-soluble carbohydrates, lignin, hemicellulose, and crude fat contents on specific biogas yield were also reported (Rath et al., 2013). In the specific case of BMP, no added value of the histological related traits was detected when these traits were jointly considered with the biochemical traits. However, it is important to keep in mind that the diversity available in sorghum was not fully covered by the present study, that crossing efforts in breeding programs will generate new diversity patterns (new trait associations...) and that breeding is a dynamic process (i.e., once the soluble sugar and mineral contents will be optimized in the elite varieties, the effects of the cell wall components on BMP will likely increase). As a consequence, the potential benefits of histological based analysis should not be ignored as they will be required in the future.

Regarding the potential of improvement of the in vitro dry matter digestibility, the key importance of the cell wall digestibility, that exhibits a larger genetic variance than IVDMD, and that depends of the composition of the cell wall (as also reported by Rodrigues et al., (2020)) but also of the spatial distribution of the tissues and of the cell wall components at the internode level was reported. These results are consistent with the ones reported in maize (El Hage et al., 2018; Legland et al., 2017) and advocate for

the development of higher throughput histological methods to facilitate breeding efforts. In terms of breeding optimization, our results also highlight the need for different sorghum stem ideotypes for methane and animal feed (as reported in maize (Rath et al., 2013)), as there is a critical need to increase sugar soluble content for methane production, whereas it needs to be controlled for animal feed to avoid elevated ethanol production in silage composition (Behling Neto et al., 2017). Whether the in vitro dry matter digestibility, or the methane potential ideotypes identified in this work need to be prioritized in the context of second-generation ethanol cultivar development for sorghum remains to be defined. However, according to the greater yield potential per unit area of structural carbohydrates (cellulose and hemicellulose) compared to soluble sugars, the first one is expected to allow higher ethanol yield per unit area. Jointly with the definition of the target ideotypes, optimized genetic gains will also depend on a better understanding of the genetic determinism of biochemical (Brenton et al., 2016; Burks et al., 2015; Hennet et al., 2020; Niu et al., 2020) and histological related traits as recently reported in maize (Mazaheri et al., 2019).

Besides the anaerobic digestion pathway that leads to biomethane production, combustion is also a strategy suitable for decentralized energy production (Van Meerbeek, Appels, Dewil, Beek, et al., 2015; Van Meerbeek, Appels, Dewil, Calmeyn, et al., 2015). According to our results, it clearly appears that different strategies will have to be deployed to breed sorghum for combustion compared to biogas production. Indeed, genetic correlations between BMP and GE are nonsignificant and for GE, the goal will be to maximize the lignin content of the cell walls as this polymer contains more gross energy than other cell wall components (Frei, 2013).

5 | CREDIT AUTHOR STATEMENT

Hélène Laurence Thomas, David Pot, and Hélène Carrère conceived the study. Céline Chauvergne, Virginie Rossard, Eric Latrille, Denis Bastianelli, Hélène Laurence Thomas, David Pot, Sylvie Jaffuel, Jean-Luc Verdeil, Christelle Baptiste, Laurent Bonnal, and Hélène Carrère involved in methodology. Eric Latrille, Denis Bastianelli, Hélène Laurence Thomas, David Pot, Sylvie Jaffuel, Jean-Luc Verdeil, Christelle Baptiste, Laurent Bonnal, and Hélène Carrère validated the study. Hélène Carrère, Hélène Laurence Thomas, and David Pot involved in formal analysis. Angélique Berger, Caroline Calatayud, Hélène Carrère, Patrice Jeanson, Joël Alcouffe, Hélène Laurence Thomas, David Pot, Sylvie Jaffuel, Jean-Luc Verdeil, and Christelle Baptiste investigated the study. Hélène Laurence Thomas and David Pot wrote the original draft. Hélène Carrère, Denis Bastianelli, Denis Bastianelli, Hélène Laurence Thomas, David Pot, Sylvie Jaffuel, Jean-Luc Verdeil, and Gilles Trouche reviewed and edited the study. Hélène Carrère, Patrice Jeanson, Joël Alcouffe, Céline Chauvergne, Virginie Rossard, Eric Latrille, Denis Bastianelli, David Pot, Jean-Luc Verdeil, Laurent Bonnal, and Gilles Trouche involved in resources of the study. David Pot and Eric Latrille involved in data curation. Hélène Carrère and David Pot obtained funding and supervised the study.

ACKNOWLEDGMENTS

This work has been funded by the "Biomass For the Future" project from the French National Research Agency (ANR, Grant ANR-11-BTBR-0006-BFF). We thank Nancy Terrier (INRAE, AGAP mixed research unit) for its careful reading of the manuscript and its suggestions of improvements. Françoise Potier (CIRAD, AGAP mixed research unit) provided a significant support to precisely define the variables used in this paper and took in charge their submission to the crop ontology website, we warmly acknowledge her for these contributions. We also wish to acknowledge the CRB GAMét (Montpellier; France, http://florilege.arcad-project.org/fr/crb/tropicales) and the USDA ARS department of the University of Nebraska, United States, for their kindness to provide us with several sorghum accessions (see Table S1).

CONFLICT OF INTEREST

The authors declare that they have no known competing financial interests or personal relationships that could have appeared to influence the work reported in this paper.

DATA AVAILABILITY STATEMENT

The data that support the findings of this study are available in the supplementary material of this article.

ORCID

David Pot https://orcid.org/0000-0001-6144-8448
Sylvie Jaffuel https://orcid.org/0000-0003-4262-1393
Jean-Luc Verdeil https://orcid.org/0000-0002-7144-9580
Christelle Baptiste https://orcid.org/0000-0001-5868-3164
Laurent Bonnal https://orcid.org/0000-0001-5038-7432
Gilles Trouche https://orcid.org/0000-0001-5408-1078
Denis Bastianelli https://orcid.org/0000-0002-6394-5920
Eric Latrille https://orcid.org/0000-0003-1717-1968
Angélique Berger https://orcid.org/0000-0003-1249-3706
Caroline Calatayud https://orcid.org/0000-0003-4910-0515

Virginie Rossard https://orcid.org/0000-0002-5484-823X
Patrice Jeanson https://orcid.org/0000-0001-8246-8026
Joël Alcouffe https://orcid.org/0000-0001-9694-6789
Hélène Carrère https://orcid.org/0000-0001-5415-9664

REFERENCES

Almeida, L. G. F. D., Parrella, R. A. D. C., Simeone, M. L. F., Ribeiro, P. C. D. O., dos Santos, A. S., da Costa, A. S. V., Guimarães, A. G., & Schaffert, R. E. (2019). Composition and growth of sorghum biomass genotypes for ethanol production. *Biomass and Bioenergy*, *122*, 343–348. https://doi.org/10.1016/j.biombioe.2019.01.030

Amaducci, S., Colauzzi, M., Battini, F., Fracasso, A., & Perego, A. (2016). Effect of irrigation and nitrogen fertilization on the production of biogas from maize and sorghum in a water limited environment. *European Journal of Agronomy*, *76*, 54–65. https://doi.org/10.1016/j.eja.2016.01.019

Arganda-Carreras, I., Kaynig, V., Rueden, C., Eliceiri, K. W., Schindelin, J., Cardona, A., & Sebastian Seung, H. (2017). Trainable Weka Segmentation: a machine learning tool for microscopy pixel classification. *Bioinformatics*, *33*, 2424–2426. https://doi.org/10.1093/bioinformatics/btx180

Aufrère, J., Baumont, R., Delaby, L., Peccatte, J.-R., Andrieu, J., Andrieu, J.-P., & Dulphy, J.-P. (2007). Laboratory prediction of forage digestibility by the pepsin-cellulase method. the renewed equations. *INRAE Productions Animals*, *20*, 129–136.

Barbanti, L., Di, G., Grigatti, M., Bertin, L., & Ciavatta, C. (2014). Anaerobic digestion of annual and multi-annual biomass crops. *Industrial Crops and Products*, *56*, 137–144. https://doi.org/10.1016/j.indcrop.2014.03.002

Behling Neto, A., Pereira, H., dos Reis, R., Silva Cabral, L., Gonçalves de Abreu, J., Sousa, D., Pedreira, B., Mombach, M., Balbinot, E., Carvalho, P., da Silva, P., & Carvalho, A. (2017). Fermentation characteristics of different purpose sorghum silage. *Semina Ciênc. Agrár.*, *38*, 2607. https://doi.org/10.5433/1679-0359.2017v38n4SUPLp2607

Bourdin, S., & Nadou, F. (2020). The role of a local authority as a stakeholder encouraging the development of biogas: A study on territorial intermediation. *Journal of Environmental Management*, *258*, 110009. https://doi.org/10.1016/j.jenvman.2019.110009

Brémond, U., Bertrandias, A., Steyer, J.-P., Bernet, N., & Carrere, H. (2020). A vision of European biogas sector development towards 2030: Trends and challenges. *Journal of Cleaner Production*, *287*, 125065. https://doi.org/10.1016/j.jclepro.2020.125065

Brenton, Z. W., Cooper, E. A., Myers, M. T., Boyles, R. E., Shakoor, N., Zielinski, K. J., Rauh, B. L., Bridges, W. C., Morris, G. P., & Kresovich, S. (2016). A genomic resource for the development, improvement, and exploitation of sorghum for bioenergy. *Genetics*, *204*, 21–33. https://doi.org/10.1534/genetics.115.183947

Burks, P. S., Kaiser, C. M., Hawkins, E. M., & Brown, P. J. (2015). Genomewide association for sugar yield in sweet Sorghum. *Crop Science*, *55*, 2138. https://doi.org/10.2135/cropsci2015.01.0057

Cai, H., Dunn, J., Wang, Z., Han, J., & Wang, M. (2013). Life-cycle energy use and greenhouse gas emissions of production of bioethanol from sorghum in the United States. *Biotechnology for Biofuels*, *6*, 141. https://doi.org/10.1186/1754-6834-6-141

Carvalho, G., & Rooney, W. L. (2017). Assessment of stalk properties to predict juice yield in Sorghum. *BioEnergy Research*, *10*, 657–670. https://doi.org/10.1007/s12155-017-9829-4

Casa, A. M., Pressoir, G., Brown, P. J., Mitchell, S. E., Rooney, W. L., Tuinstra, M. R., Franks, C. D., & Kresovich, S. (2008). Community resources and strategies for association mapping in Sorghum. *Crop Science*, *48*, 30. https://doi.org/10.2135/cropsci2007.02.0080

Chauvergne, C., Bonnal, L., Bastianelli, D., Carrère, H., Griveau, Y., Jacquemot, M.-P., Reymond, M., Méchin, V., Rossard, V., & Latrille, É. (2020). Dataset of organic sample near infrared spectra acquired on different spectrometers. *Data Brief*, *32*, 106264. https://doi.org/10.1016/j.dib.2020.106264

El Hage, F., Legland, D., Borrega, N., Jacquemot, M.-P., Griveau, Y., Coursol, S., Méchin, V., & Reymond, M. (2018). Tissue lignification, cell wall p-coumaroylation and degradability of maize stems depend on water status. *Journal of Agriculture and Food Chemistry*, *66*, 4800–4808. https://doi.org/10.1021/acs.jafc.7b05755

Fertitta-Roberts, C., Spatari, S., Grantz, D. A., & Jenerette, G. D. (2017). Trade-offs across productivity, GHG intensity, and pollutant loads from second-generation sorghum bioenergy. *GCB Bioenergy*, *9*, 1764–1779. https://doi.org/10.1111/gcbb.12471

Frei, M. (2013). Lignin: characterization of a multifaceted crop component. *Scientific World Journal*, *2013*, 1–25. https://doi.org/10.1155/2013/436517

Fulton-Smith, S., & Cotrufo, M. F. (2019). Pathways of soil organic matter formation from above and belowground inputs in a Sorghum bicolor bioenergy crop. *GCB Bioenergy*, *11*, 971–987. https://doi.org/10.1111/gcbb.12598

Garuti, M., Mantovi, P., Soldano, M., Immovilli, A., Ruozzi, F., Fermoso, F. G., Rodriguez, A. J., & Fabbri, C. (2020). Towards sustainable energy-crop cultivation: feasibility of biomethane production using a double-cropping system with various sorghum phenotypes. *Biofuels, Bioproducts and Biorefining*, *14*, 553–565. https://doi.org/10.1002/bbb.2099

Gautam, S., Mishra, U., Scown, C. D., & Zhang, Y. (2020). Sorghum biomass production in the continental United States and its potential impacts on soil organic carbon and nitrous oxide emissions. *GCB Bioenergy*, *12*, 878–890. https://doi.org/10.1111/gcbb.12736

Gomez, F. E., Carvalho, G., Shi, F., Muliana, A. H., & Rooney, W. L. (2018). High throughput phenotyping of morpho-anatomical stem properties using X-ray computed tomography in sorghum. *Plant Methods*, *14*, 59. https://doi.org/10.1186/s13007-018-0326-3

Gómez-de-Mariscal, E., García-López-de-Haro, C., & Donati, L. (2019). DeepImageJ: A user-friendly plugin to run deep learning models in ImageJ 13.

Guden, B., Erdurmus, C., Erdal, S., & Uzun, B. (2020). Evaluation of sweet sorghum genotypes for bioethanol yield and related traits. *Biofuels, Bioproducts and Biorefining*, *15*(2), 545–562. https://doi.org/10.1002/bbb.2169

Hao, B., Xue, Q., Bean, B. W., Rooney, W. L., & Becker, J. D. (2014). Biomass production, water and nitrogen use efficiency in photoperiod-sensitive sorghum in the Texas High Plains. *Biomass and Bioenergy*, *62*, 108–116. https://doi.org/10.1016/j.biombioe.2014.01.008

Hennet, L., Berger, A., Trabanco, N., Ricciuti, E., Dufayard, J.-F., Bocs, S., Bastianelli, D., Bonnal, L., Roques, S., Rossini, L., Luquet, D., Terrier, N., & Pot, D. (2020). Transcriptional regulation of sorghum stem composition: key players identified

through co-expression gene network and comparative genomics analyses. *Frontiers in Plant Science*, *11*, https://doi.org/10.3389/fpls.2020.00224

Jankowski, K. J., Dubis, B., Sokólski, M. M., Załuski, D., Bórawski, P., & Szempliński, W. (2020). Productivity and energy balance of maize and sorghum grown for biogas in a large-area farm in Poland: an 11-year field experiment. *Industrial Crops and Products*, *148*, 112326. https://doi.org/10.1016/j.indcrop.2020.112326

Legland, D., El-Hage, F., Méchin, V., & Reymond, M. (2017). Histological quantification of maize stem sections from FASGA-stained images. *Plant Methods*, *13*, 84. https://doi.org/10.1186/s13007-017-0225-z

Lesteur, M., Latrille, E., Maurel, V. B., Roger, J. M., Gonzalez, C., Junqua, G., & Steyer, J. P. (2011). First step towards a fast analytical method for the determination of Biochemical Methane Potential of solid wastes by near infrared spectroscopy. *Bioresource Technology*, *102*, 2280–2288. https://doi.org/10.1016/j.biortech.2010.10.044

Liu, H., Ren, L., Spiertz, H., Zhu, Y., & Xie, G. H. (2015). An economic analysis of sweet sorghum cultivation for ethanol production in North China. *GCB Bioenergy*, *7*, 1176–1184. https://doi.org/10.1111/gcbb.12222

Luquet, D., Perrier, L., Clément-Vidal, A., Jaffuel, S., Verdeil, J.-L., Roques, S., Soutiras, A., Baptiste, C., Fabre, D., Bastianelli, D., Bonnal, L., Sartre, P., Rouan, L., & Pot, D. (2019). Genotypic covariations of traits underlying sorghum stem biomass production and quality and their regulations by water availability: Insight from studies at organ and tissue levels. *GCB Bioenergy*, *11*, 444–462. https://doi.org/10.1111/gcbb.12571

Mahmood, A., & Honermeier, B. (2012). Chemical composition and methane yield of sorghum cultivars with contrasting row spacing. *Field Crops Research*, *128*, 27–33. https://doi.org/10.1016/j.fcr.2011.12.010

Mahmood, A., Ullah, H., Ijaz, M., Javaid, M., Shahzad, A., & Honermeier, B. (2013). Evaluation of sorghum hybrids for biomass and biogas production. *Australian Journal of Crop Science*, *7*, 1456–1462.

Mazaheri, M., Heckwolf, M., Vaillancourt, B., Gage, J. L., Burdo, B., Heckwolf, S., Barry, K., Lipzen, A., Ribeiro, C. B., Kono, T. J. Y., Kaeppler, H. F., Spalding, E. P., Hirsch, C. N., Robin Buell, C., de Leon, N., & Kaeppler, S. M. (2019). Genome-wide association analysis of stalk biomass and anatomical traits in maize. *BMC Plant Biology*, *19*, 45. https://doi.org/10.1186/s12870-019-1653-x

Mitchell, R. B., Schmer, M. R., Anderson, W. F., Jin, V., Balkcom, K. S., Kiniry, J., Coffin, A., & White, P. (2016). Dedicated energy crops and crop residues for bioenergy feedstocks in the central and eastern USA. *BioEnergy Research*, *9*, 384–398. https://doi.org/10.1007/s12155-016-9734-2

Monlau, F., Sambusiti, C., Barakat, A., Guo, X. M., Latrille, E., Trably, E., Steyer, J.-P., & Carrere, H. (2012). Predictive models of biohydrogen and biomethane production based on the compositional and structural features of lignocellulosic materials. *Environmental Science and Technology*, *46*, 12217–12225. https://doi.org/10.1021/es303132t

Moore, C. E., von Haden, A. C., Burnham, M. B., Kantola, I. B., Gibson, C. D., Blakely, B. J., Dracup, E. C., Masters, M. D., Yang, W. H., DeLucia, E. H., & Bernacchi, C. J. (2021). Ecosystem-scale biogeochemical fluxes from three bioenergy crop candidates: How energy sorghum compares to maize and miscanthus. *GCB Bioenergy*, *13*, 445–458. https://doi.org/10.1111/gcbb.12788

Niu, H., Ping, J., Wang, Y., Lv, X., Li, H., Zhang, F., Chu, J., & Han, Y. (2020). Population genomic and genome-wide association analysis of lignin content in a global collection of 206 forage sorghum accessions. *Molecular Breeding*, *40*, 73. https://doi.org/10.1007/s11032-020-01151-7

Oikawa, P. Y., Jenerette, G. D., & Grantz, D. A. (2015). Offsetting high water demands with high productivity: Sorghum as a biofuel crop in a high irradiance arid ecosystem. *GCB Bioenergy*, *7*, 974–983. https://doi.org/10.1111/gcbb.12190

Pasteris, A. M., Zapka, O., Plogsties, V., Herrmann, C., & Heiermann, M. (2021). Effects of sorghum biomass quality on ensilability and methane yield. *GCB Bioenergy*, *13*(5), 803–822. https://doi.org/10.1111/gcbb.12814

Perrier, L., Rouan, L., Jaffuel, S., Clément-Vidal, A., Roques, S., Soutiras, A., Baptiste, C., Bastianelli, D., Fabre, D., Dubois, C., Pot, D., & Luquet, D. (2017). Plasticity of sorghum stem biomass accumulation in response to water deficit: a multiscale analysis from internode tissue to plant level. *Frontiers in Plant Science*, *8*, 1516. https://doi.org/10.3389/fpls.2017.01516

R Core Team (2018). *R: A language and environment for statistical computing*. R Foundation for Statistical Computing.

Rath, J., Heuwinkel, H., & Herrmann, A. (2013). Specific biogas yield of maize can be predicted by the interaction of four biochemical constituents. *BioEnergy Research*, *6*(3), 939–952. https://doi.org/10.1007/s12155-013-9318-3

Rezende, M. L., & Richardson, J. W. (2017). Risk analysis of using sweet sorghum for ethanol production in southeastern Brazil. *Biomass and Bioenergy*, *97*, 100–107. https://doi.org/10.1016/j.biombioe.2016.12.016

Rodrigues, P. H. M., Pinedo, L. A., Meyer, P. M., da Silva, T. H., da Guimarães, I. C. S. B. (2020). Sorghum silage quality as determined by chemical–nutritional factors. *Grass & Forage Science*, *75*, 462–473. https://doi.org/10.1111/gfs.12495

Rooney, W. L., Blumenthal, J., Bean, B., & Mullet, J. E. (2007). Designing sorghum as a dedicated bioenergy feedstock. *Biofuels, Bioproducts and Biorefining*, *1*, 147–157. https://doi.org/10.1002/bbb.15

Saballos, A. (2008). Development and utilization of Sorghum as a bioenergy crop. In *Genetic improvement of bioenergy crops*. Springer. https://doi.org/10.1007/978-0-387-70805

Salih, A. A., Ali, I. A., Lux, A., Luxova, M., Cohen, Y., Sugimoto, Y., & Inanaga, S. (1999). Rooting, water uptake, and xylem structure adaptation to drought of two sorghum cultivars. *Crop Science*, *39*, 168–173. https://doi.org/10.2135/cropsci1999.0011183X003900010027x

Sambusiti, C., Monlau, F., Ficara, E., Carrère, H., & Malpei, F. (2013). A comparison of different pre-treatments to increase methane production from two agricultural substrates. *Applied Energy*, *104*, 62–70. https://doi.org/10.1016/j.apenergy.2012.10.060

Shoemaker, C., & Bransby, D. (2010). The role of sorghum as a bioenergy feedstock. *Sustainable alternative fuel feedstock opportunities, challenges and roadmaps for six US regions* (pp. 149–159). Soil and Water Conservation Society.

Shu, K., Kozak, M., Fradj, N. B., Zylowski, T., & Rozakis, S. (2020). Simulation of sorghum introduction and its impacts on land use change—A case study on Lubelski region of Eastern Poland. *GCB Bioenergy*, *12*, 252–274. https://doi.org/10.1111/gcbb.12669

Szambelan, K., Nowak, J., Frankowski, J., Szwengiel, A., Jeleń, H., & Burczyk, H. (2018). The comprehensive analysis of sorghum cultivated in Poland for energy purposes: Separate hydrolysis and fermentation and simultaneous saccharification and fermentation methods and their impact on bioethanol effectiveness and volatile by-products from the grain and the energy potential of sorghum straw. *Bioresource Technology*, *250*, 750–757. https://doi.org/10.1016/j.biortech.2017.11.096

Thomas, H. L., Pot, D., Latrille, E., Trouche, G., Bonnal, L., Bastianelli, D., & Carrère, H. (2017). Sorghum Biomethane Potential Varies with the Genotype and the Cultivation Site. *Waste Biomass Valorization*, *10*(4), 783–788. https://doi.org/10.1007/s12649-017-0099-3

Tolivia, D., & Tolivia, J. (1987). Fasga: A new polychromatic method for simultaneous and differential staining of plant tissues. *Journal of Microscopy*, *148*, 113–121. https://doi.org/10.1111/j.1365-2818.1987.tb02859.x

Trouche, G., Bastianelli, D., Hamadou, T. V. C., Chantereau, J., Rami, J.-F., & Pot, D. (2014). Exploring the variability of a photoperiod-insensitive sorghum genetic panel for stem composition and related traits in temperate environments. *Field Crops Research*, *166*, 72–81. https://doi.org/10.1016/j.fcr.2014.06.008

Tsuchihashi, N., & Goto, Y. (2005). Internode characteristics of sweet sorghum (*Sorghum bicolor* (L.) Moench) during dry and rainy seasons in Indonesia. *Plant Prod. Sci.*, *8*, 601–607. https://doi.org/10.1626/pps.8.601

Van Meerbeek, K., Appels, L., Dewil, R., Beek, J. V., Bellings, L., Liebert, K., Muys, B., & Hermy, M. (2015). Energy potential for combustion and anaerobic digestion of biomass from low-input high-diversity systems in conservation areas. *GCB Bioenergy*, *7*, 888–898. https://doi.org/10.1111/gcbb.12208

Van Meerbeek, K., Appels, L., Dewil, R., Calmeyn, A., Lemmens, P., Muys, B., & Hermy, M. (2015). Biomass of invasive plant species as a potential feedstock for bioenergy production. *Biofuels, Bioproducts and Biorefining*, *9*(3), 273–282, https://doi.org/10.1002/bbb.1539

Van Soest, P. J., Robertson, J. B., & Lewis, B. A. (1991). Methods for dietary fiber, neutral detergent fiber, and nonstarch polysaccharides in relation to animal nutrition. *Journal of Dairy Science*, *74*, 3583–3597. https://doi.org/10.3168/jds.S0022-0302(91)78551-2

Vandenbrink, J. P., Delgado, M. P., Frederick, J. R., & Feltus, F. A. (2010). A sorghum diversity panel biofuel feedstock screen for genotypes with high hydrolysis yield potential. *Industrial Crops and Products*, *31*, 444–448. https://doi.org/10.1016/j.indcrop.2010.01.001

Vandenbrink, J. P., Hammonds, R. E., Hilten, R. N., Das, K. C., Henson, J. M., Paterson, A. H., & Feltus, F. A. (2013). Tissue specific analysis of bioconversion traits in the bioenergy grass Sorghum bicolor. *Industrial Crops and Products*, *50*, 118–130. https://doi.org/10.1016/j.indcrop.2013.06.039

Vlachos, C. E., Mariolis, N. A., & Skaracis, G. N. (2015). A comparison of sweet sorghum and maize as first-generation bioethanol feedstocks in Greece. *Journal of Agricultural Science*, *153*, 853–861. https://doi.org/10.1017/S0021859614000446

Vries, S. C. D., Ven, G. W. J. V. D., Ittersum, M. K. V., & Giller, K. E. (2012). The production-ecological sustainability of cassava, sugarcane and sweet sorghum cultivation for bioethanol in Mozambique. *GCB Bioenergy*, *4*, 20–35. https://doi.org/10.1111/j.1757-1707.2011.01103.x

Windpassinger, S., Friedt, W., Frauen, M., Snowdon, R., & Wittkop, B. (2015). Designing adapted sorghum silage types with an enhanced energy density for biogas generation in temperate Europe. *Biomass and Bioenergy*, *81*, 496–504. https://doi.org/10.1016/j.biombioe.2015.08.005

Xia, J., Zhao, Y., Burks, P., Pauly, M., & Brown, P. J. (2018). A sorghum NAC gene is associated with variation in biomass properties and yield potential. *Plant Direct*, *2*, e00070. https://doi.org/10.1002/pld3.70

Xu, N., Liu, S., Xin, F., Zhou, J., Jia, H., Xu, J., Jiang, M., & Dong, W. (2019). Biomethane production from lignocellulose: Biomass recalcitrance and its impacts on anaerobic digestion. *Frontiers in Bioengineering and Biotechnology*, *7*, https://doi.org/10.3389/fbioe.2019.00191

Zegada-Lizarazu, W., Luna, D. F., & Monti, A. (2015). Photosynthetic acclimation of sweet sorghum under progressive water stress. *Industrial Crops and Products*, *66*, 216–219. https://doi.org/10.1016/j.indcrop.2014.12.045

SUPPORTING INFORMATION

Additional supporting information may be found online in the Supporting Information section.

How to cite this article: Thomas, H. L., Pot, D., Jaffuel, S., Verdeil, J.-L., Baptiste, C., Bonnal, L., Trouche, G., Bastianelli, D., Latrille, E., Berger, A., Calatayud, C., Chauvergne, C., Rossard, V., Jeanson, P., Alcouffe, J., & Carrère, H. (2021). Mobilizing sorghum genetic diversity: Biochemical and histological-assisted design of a stem ideotype for biomethane production. *GCB Bioenergy*, 00, 1–20. https://doi.org/10.1111/gcbb.12886